

The Perturbative and Non-Perturbative Interface

MINER ν A Note 500, November 2004

Cynthia Keppel, Hampton University and Jefferson Lab
Ioana Niculescu, James Madison University
Gabriel Niculescu, James Madison University

November 17, 2004

Abstract

The nature of the transition from nonperturbative, strongly coupled QCD at low energy to perturbative QCD at high energy is a central mystery in hadron and nuclear physics. This document elucidates the key roles that the MINER ν A experiment will play in studying this topic.

Three decades after the establishment of QCD as the theory of the strong nuclear force, understanding *how* QCD works remains one of the great challenges in nuclear physics. A major obstacle arises from the fact that the degrees of freedom observed in nature (hadrons and nuclei) are totally different from those appearing in the QCD Lagrangian (current quarks and gluons). The remarkable feature of QCD at large distances — quark confinement — prevents the individual quark and gluon constituents making up hadronic bound states to be removed and examined in isolation. Making the transition from quark and gluon to hadron degrees of freedom is therefore the key to our ability to describe nature from first principles.

Experimentally, understanding this transition requires reliable data in three kinematic regimes: in the scaling domain of high Q^2 deep inelastic scattering; in the hadronic region of resonances and quasi-elastic scattering; and, perhaps most importantly, in the moderate Q^2 region between the two, where the transition is made manifest most dramatically. MINER ν A is uniquely situated to address this compelling topic for the first time with neutrinos. As can be seen in Figure 1, this pioneering measurement will span all three regimes, and will provide crucial data in the transition region.

Despite the apparent dichotomy between the partonic and hadronic regimes, in nature there exist instances where the behavior of low-energy cross sections, averaged over appropriate energy intervals, closely resembles that at asymptotically high energies, calculated in terms of quark-gluon degrees of freedom. This phenomenon is referred to as *quark-hadron duality*, and reflects the relationship between confinement and asymptotic freedom, and the

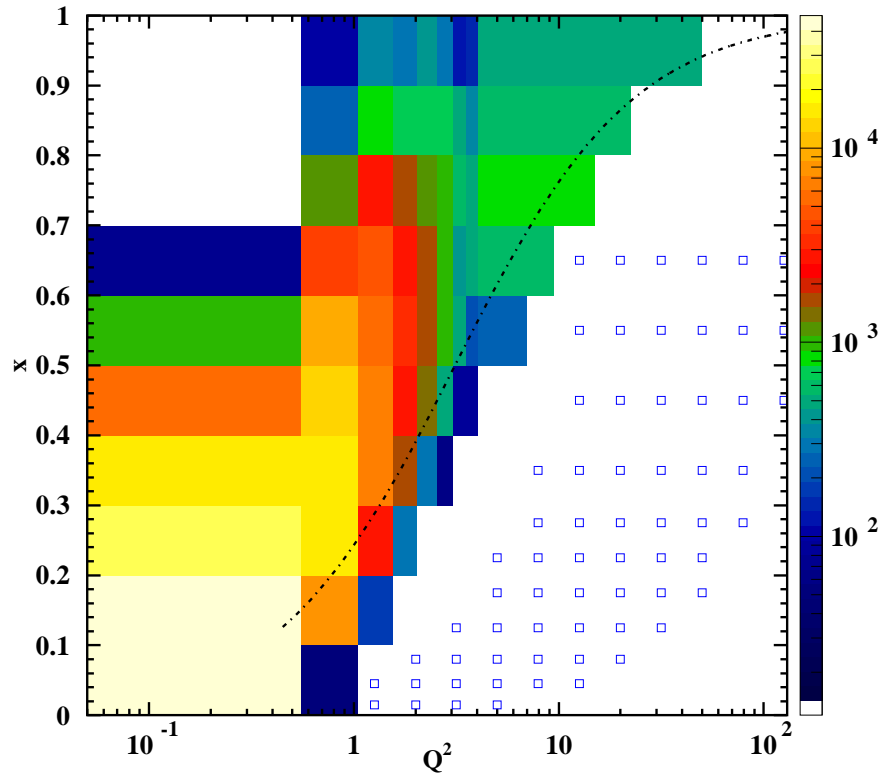


Figure 1: Kinematics plot in x (Bjorken) versus Q^2 of the available xF_3 data (open symbols) and the anticipated (resonance region) Minerva data (colored distributions). The curve indicates the commonly-accepted $W^2 = 4 \text{ GeV}^2$ boundary between the resonance and deep inelastic regimes. The color key to the right shows the corresponding, expected Minerva statistics.

transition from perturbative to nonperturbative regimes in QCD. Such duality is in fact quite general, and arises in many different physical processes, such as in e^+e^- annihilation into hadrons, or semi-leptonic decays of heavy mesons.

In electron–nucleon scattering, quark-hadron duality links the physics of resonance production to the physics of scaling, and is the focus of substantial renewed interest in understanding the structure of the nucleon [1, 2, 3, 4, 5]. For example, there are over 10 approved experiments at Jefferson Lab which address this topic, and it is a major focus area of the planned energy upgrade at this laboratory. Figure 2 demonstrates duality in the F_2 structure function measured at Jefferson Lab [1], for the nucleon and for nuclei. In all, data in the (hadronic) resonance region average to the perturbative scaling prediction, most dramatically in the nucleus where Fermi motion facilitates the required averaging completely and the partonic curve and hadronic data are indistinguishable.

Weak currents can provide complementary information on the quark structure of hadrons, not accessible to electromagnetic probes. In particular, neutrino-induced reactions can provide important consistency checks on the validity of duality. While deep inelastic neutrino structure functions are determined by the same set of universal parton distribution functions as in charged lepton scattering, the structure of resonance transitions excited by neutrino beams is in some cases strikingly different to that excited by virtual photons. Although on general grounds one may expect that a duality should also exist for weak structure functions [6], the details of how this manifests itself in neutrino scattering may be quite different from that observed in electron scattering.

The main difference between electron and neutrino scattering reactions can be most easily understood by considering specific resonance transitions. While a neutrino beam can convert a neutron into a proton, it cannot convert a proton into a neutron, for example (and *vice versa* for an antineutrino beam). Similarly, there are dramatic differences between inelastic production rates in the Δ resonance region [7, 8] — because of charge conservation, only transitions to isospin-3/2 states from the proton are allowed.

Unfortunately, current neutrino scattering data are sparse in the resonance region [9], and, due to the small weak cross sections, are often only available for heavy nuclei (where large target volumes are easier to handle and are more affordable than light nuclei) [10]. It has not therefore been possible to make any concrete statements to date about the validity of duality in neutrino scattering.

The prospect of high-intensity neutrino beams at Fermilab, offers a valuable complement to the study of duality and resonance transitions of current interest in electron scattering. MINER ν A will be an exceptional tool for such measurements. The goal of MINER ν A, to perform a high-statistics neutrino-nucleus scattering experiments using a fine-grained detector specifically designed to measure low-energy neutrino-nucleus interactions accurately, over both the resonance and deep inelastic regimes, will make MINER ν A the premiere facility to study quark-hadron duality in neutrino scattering.

Aside from studying quark-hadron duality, an obvious motivation for additional neutrino structure function measurements is the crucial role played by neutrino scattering

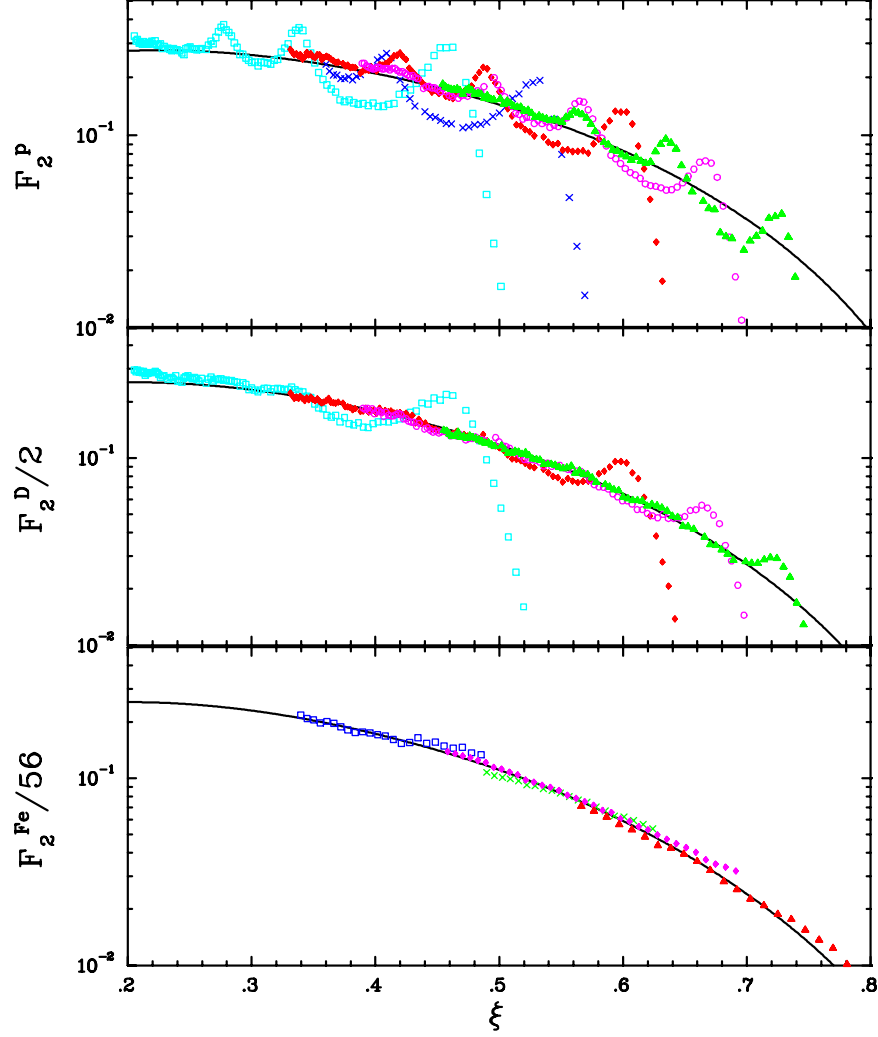


Figure 2: F_2 structure function per nucleon vs ξ (the Nachtmann scaling variable, accounting for target mass effects) for hydrogen (top), deuterium, and iron (bottom). The data are all in the resonance region. The curves are the GRV pdf-based, perturbative parameterization at $Q^2 = 1.0 \text{ GeV}^2$, corrected for the EMC effect. Uncertainties shown are statistical only.

physics in the extraction of the fundamental parton distribution functions (pdfs). The pdfs give the number of partons (quarks and gluons) in a proton or other hadron, and (in the "MS-bar" convention) are precisely defined in terms of matrix elements of operators. One of the most compelling examples of the necessity of neutrino results in nucleon structure studies is the ability to extract pdfs and to directly resolve the flavor of the nucleonic constituents: ν interacts with d , s , \bar{u} and \bar{c} while the $\bar{\nu}$ interacts with u , c , \bar{d} and \bar{s} . This unique ability of the neutrino to "taste" only particular flavors of quarks significantly enhances the study of parton distribution functions. A high-statistics study of the partonic structure of the nucleon is here proposed, using the neutrino's weak probe, to complement the on-going study of this subject with electromagnetic probes at other laboratories.

With the high statistics, as well as the special attention to minimizing neutrino beam systematics, it should be possible for the first time with MINER ν A to eventually determine the separate structure functions $F_1^{\nu N}(x, Q^2)$, $F_1^{\bar{\nu} N}(x, Q^2)$, $F_2^{\nu N}(x, Q^2)$, $F_2^{\bar{\nu} N}(x, Q^2)$, $xF_3^{\nu N}(x, Q^2)$ and $xF_3^{\bar{\nu} N}(x, Q^2)$ where N is an isoscalar target. As an example, in leading order QCD (used for illustrative purposes), four of the structure functions are related to the parton distribution functions by:

$$\begin{aligned}
2F_1^{\nu N}(x, Q^2) &= u(x) + d(x) + s(x) + \bar{u}(x) + \bar{d}(x) + \bar{c}(x) \\
2F_1^{\bar{\nu} N}(x, Q^2) &= u(x) + d(x) + c(x) + \bar{u}(x) + \bar{d}(x) + \bar{s}(x) \\
xF_3^{\nu N}(x, Q^2) &= u(x) + d(x) + s(x) - \bar{u}(x) - \bar{d}(x) - \bar{c}(x) \\
xF_3^{\bar{\nu} N}(x, Q^2) &= u(x) + d(x) + c(x) - \bar{u}(x) - \bar{d}(x) - \bar{s}(x)
\end{aligned}$$

Note that taking differences and sums of these structure functions allows extraction of individual parton distribution functions in a given x , Q^2 bin. For example:

$$\begin{aligned}
2F_1^{\nu N} - 2F_1^{\bar{\nu} N} &= [s(x) - \bar{s}(x)] + [\bar{c}(x) - c(x)] \\
2F_1^{\nu N} - xF_3^{\nu N} &= 2[\bar{u}(x) + \bar{d}(x) + \bar{c}(x)] \\
2F_1^{\bar{\nu} N} - xF_3^{\bar{\nu} N} &= 2[\bar{u}(x) + \bar{d}(x) + \bar{s}(x)] \\
xF_3^{\nu N} - xF_3^{\bar{\nu} N} &= [\bar{s}(x) + s(x)] - [\bar{c}(x) + c(x)]
\end{aligned}$$

With the manageable systematic uncertainties expected, the ability to isolate individual parton distribution functions will be dramatically increased by measuring the full set of separate ν and $\bar{\nu}$ structure functions with this experiment. There are two primary (associated) methods for extracting this full set of structure functions. One can either use the varying y behavior of the coefficients of the structure functions in the expression for the cross section:

$$\begin{aligned} \frac{d^2\sigma^{\nu(\bar{\nu})}}{dxdy} = & 2\frac{G_F^2 M_p E_\nu}{\pi} \left[xy^2 F_1^{\nu(\bar{\nu})}(x, Q^2) + \right. \\ & \left(1 - y - \frac{M_p xy}{2E_\nu}\right) F_2^{\nu(\bar{\nu})}(x, Q^2) \pm \\ & \left. y(1 - y/2) x F_3^{\nu(\bar{\nu})}(x, Q^2) \right], \end{aligned}$$

or one can use the "helicity representation" of the cross section:

$$\begin{aligned} \frac{d^2\sigma^\nu}{dxdQ^2} = & \frac{G_F^2}{2\pi x} \left[\frac{1}{2} (F_2^\nu(x, Q^2) + x F_3^\nu(x, Q^2)) + \right. \\ & \frac{(1-y)^2}{2} (F_2^\nu(x, Q^2) - x F_3^\nu(x, Q^2)) - \\ & \left. 2y^2 F_L^\nu(x, Q^2) \right], \end{aligned}$$

and

$$\begin{aligned} \frac{d^2\sigma^{\bar{\nu}}}{dxdQ^2} = & \frac{G_F^2}{2\pi x} \left[\frac{1}{2} (F_2^{\bar{\nu}}(x, Q^2) - x F_3^{\bar{\nu}}(x, Q^2)) + \right. \\ & \frac{(1-y)^2}{2} (F_2^{\bar{\nu}}(x, Q^2) + x F_3^{\bar{\nu}}(x, Q^2)) - \\ & \left. 2y^2 F_L^{\bar{\nu}}(x, Q^2) \right], \end{aligned}$$

By plotting events as a function of $(1-y)^2$ in a given x, Q^2 bin, it is possible to extract all six structure functions. We note that, for this sort of parton distribution function study, good statistics for anti-neutrino running are an imperative.

Systematic uncertainties in extracting the $x F_3$ structure function have been studied. The dominant source of systematic uncertainty is the determination of incident neutrino energy. In the MINER ν A experiment this energy is determined indirectly, by summing up the energies deposited by outgoing hadrons in the hadronic calorimeter (E_{HAD}), and then adding the energy of the outgoing muon:

$$E_\nu = E_{HAD} + E_\mu - M, \quad (1)$$

where M is the nucleon mass. The uncertainty in the neutrino energy is therefore dominated by the resolution of the hadronic calorimeter. For the resonance kinematic regime this

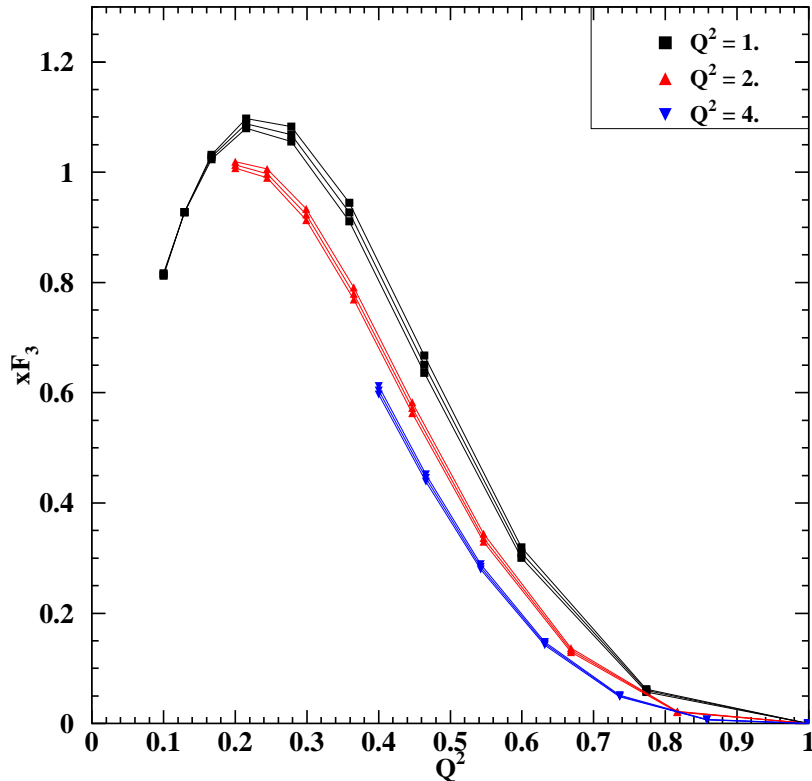


Figure 3: Variation in xF_3 due to the uncertainty on the four momentum transfer, as described in the text.

resolution was determined to be $20\% / \sqrt{E_{HAD}}$, with E_{HAD} in GeV. This variation amounts to an uncertainty of 4–7 % in the four momentum transfer, Q^2 . The CTEQ6M model was used to generate parton distribution functions, from which a projected xF_3 structure function was computed. Results are shown in Figure 3 for three nominal Q^2 values (1, 2, and 4 GeV^2), with Q^2 varying by 7 % around the nominal value.

While the variations shown in Figure 3 are rather small, xF_3 is not directly accessible experimentally. What will be measured in practice are yields, from which differential cross-sections will be calculated. As discussed above, the neutrino/antineutrino differential cross-section can be expanded as a linear combination of structure functions. The colored bands shown in Figure 4 represent the expected variation in xF_3 when the E_{HAD} dependence of all the kinematic factors from equation 1 are taken into account. This is likely a conservative overestimate of the uncertainty, since the energy resolution uncertainty is being multiply counted. Even with this, though, it is clear that precise data will be available in the pivotal large x region.

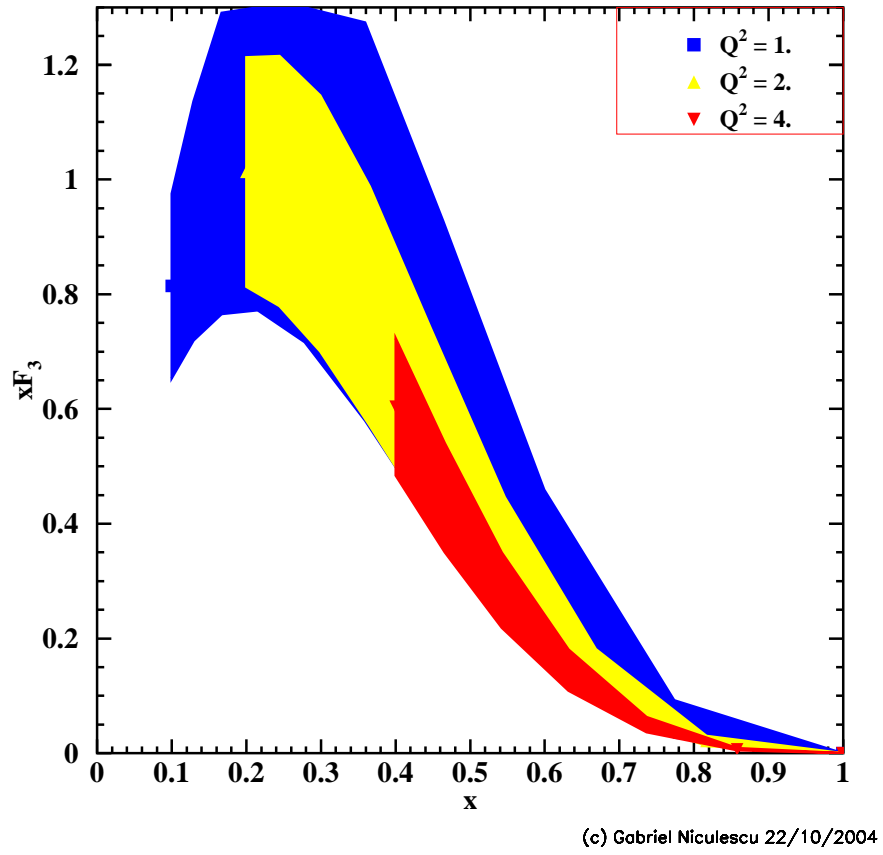


Figure 4: Expected uncertainties for xF_3 extracted from differential cross-sections, as described in the text.

We note that the fully active region of the Minerva detector provides an enormous amount of information for each neutrino interaction. The fine segmentation of the fully active region provides excellent capabilities for topological identification, and the optical system and readout electronics are designed to provide accurate position, pulse height, and timing information for each strip crossing to further enhance the detector's particle identification and reconstruction capabilities. Unfortunately, making full use of this abundance of information requires highly sophisticated pattern recognition software, the development of which typically takes person-years and inevitably becomes one of the main areas of activity once an experiment moves out of the design/construction phase. The reconstruction developed for the proposal studies, while sufficient to address a number of important questions for the overall design of the experiment, was not optimized for the analyzes described here. It is certain that a final, fully optimized reconstruction that includes particle-by-particle reconstruction for low multiplicity final states will have markedly better resolution than that quoted here.

Going beyond leading-order QCD and taking gluons into consideration, we need to bring global fitting techniques into the extraction of the parton distribution functions. The QCD evolution of parton distribution functions takes high- x_{Bj} pdfs at low Q^2 and evolves them down to moderate-and-low x at higher Q^2 . This means that one of the larger contributions to background uncertainties at, for instance, LHC measurements will be the very poorly known high- x pdfs at the lower Q^2 values open to NuMI neutrino beams. One problem in studying this point has been the accumulation of sufficient statistics at high x , off of light targets, to extract the pdfs. As can be seen in Figure 1 MINER ν A will sit in the optimal kinematic region and will yield the necessary statistics to start addressing this major concern.

Both global fitting efforts and MINER ν A data analysis will benefit from the large overlap between the Jefferson Lab and MINER ν A kinematic regimes. High precision structure function measurements at Jefferson Lab over the same x and Q^2 ranges as MINER ν A will provide valuable constraints on the vector coupling in extracting structure functions and pdfs from MINER ν A data. Another example is the role which will be played by Jefferson Lab in disentangling the nuclear effects required to obtain nucleon information from nuclear targets. As one example, Figure 5, depicting the same A -dependence in low Q^2 structure function data from Jefferson Lab in the resonance regime and high Q^2 deep inelastic data from CERN and SLAC [11], suggests that the nuclear dependence of the structure functions, an easily parameterizable if not well understood effect, should be the same in the frontier MINER ν A kinematic range as in the well-measured DIS regime. Other Jefferson Lab experiments will directly address additional relevant issues, such as final state interactions and on-shell extrapolation, all of which are particularly important at large x .

Although a large body of structure function data exists over a wide range of x and Q^2 , the region $x > 0.6$ is not well explored. As discussed above, a precision investigation of this large x regime in neutrino scattering will be made possible for the first time with MINER ν A. For $x \geq 0.4$ the contributions from the $q\bar{q}$ sea become negligible, and the structure functions

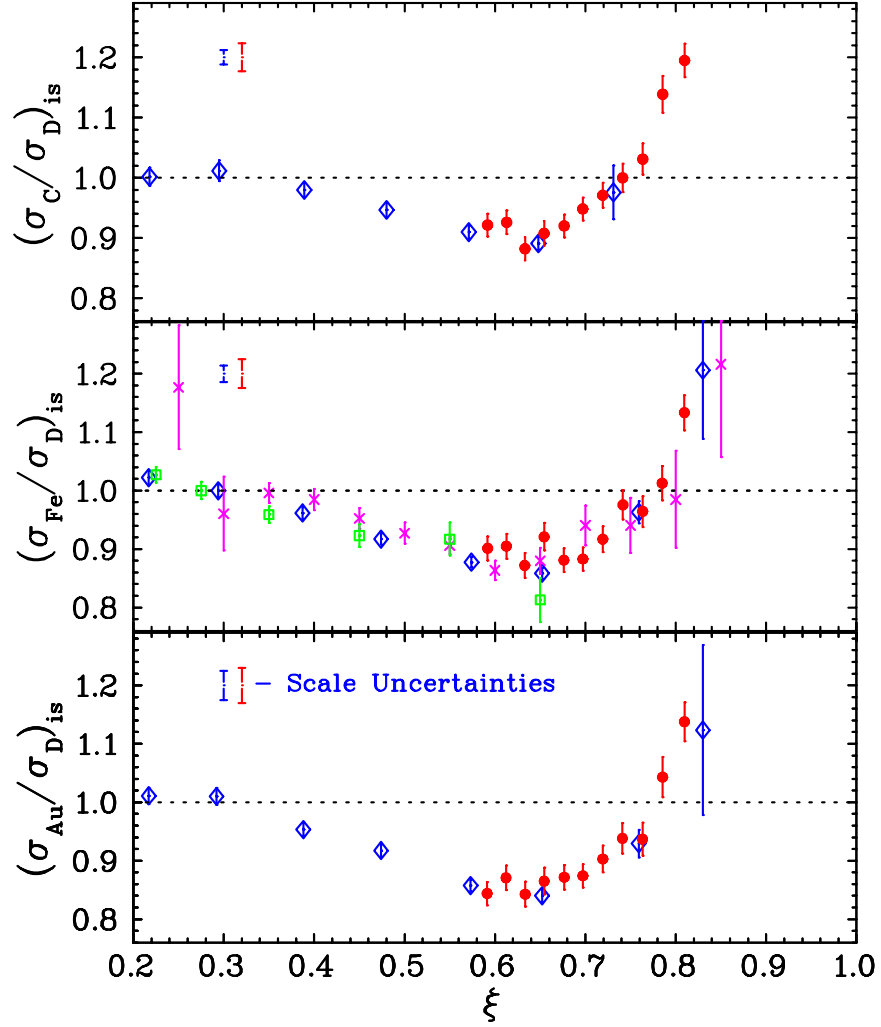


Figure 5: Ratio of nuclear to deuterium cross sections per nucleon, corrected for neutron excess, for Carbon (top), Iron (center) and Gold (bottom) versus ξ . The resonance data at low W and Q^2 from Jefferson Lab (circles) are compared with the deep inelastic data at high W and Q^2 from SLAC E139 (diamonds), SLAC E87 (crosses), and BCDMS (squares). The scale uncertainties for the SLAC (left) and JLab (right) data are shown in the figure.

are dominated by the valence quarks. Knowledge of the valence quark distributions of the nucleon at large x is vital for several reasons. The simplest SU(6) symmetric quark model predicts that the ratio of d to u quark distributions in the proton is $1/2$, however, the breaking of this symmetry in nature results in a much smaller ratio. Various mechanisms have been invoked to explain why the $d(x)$ distribution is softer than $u(x)$. If the interaction between quarks that are spectators to the deep inelastic collision is dominated by one-gluon exchange, for instance, the d quark distribution will be suppressed, and the d/u ratio will tend to zero in the limit $x \rightarrow 1$ [12]. This assumption has been built into most global analyzes of parton distribution functions, but has never been tested independently. On the other hand, if the dominant reaction mechanism involves deep inelastic scattering from a quark with the same spin orientation as the nucleon, as predicted by perturbative QCD counting rules, then d/u tends to $\approx 1/5$ as $x \rightarrow 1$ [13]. Measurements of structure functions at large x will bring insights into the mechanisms responsible for spin-flavor symmetry breaking.

In addition, quark distributions at large x are a crucial input for estimating backgrounds in searches for new physics beyond the Standard Model at high energy colliders [14]. The QCD evolution of parton distribution functions takes high- x_{Bj} pdfs at low Q^2 and evolves them down to moderate-and-low x at higher Q^2 . This obviously means that one of the larger contributions to background uncertainties at LHC measurements will be the very poorly known high- x pdfs at the lower Q^2 values open to NuMI neutrino beams. That there appears to be an unexplained anomaly at high x will be discussed below. We note first that one problem in studying this point with neutrinos has been the accumulation of sufficient statistics at high x , off of light targets, to extract the pdfs. MINER ν A will yield the necessary data to start addressing this major concern.

The uncertainties in the current nucleon parton distribution functions at high x are of two types: the ratio of the light quark pdfs, $d(x)/u(x)$, as $x \rightarrow 1$ and the role of leading power corrections (higher twist) in the extraction of the high x behavior of the quarks. Analyzes of present leptonproduction data sets that used hydrogen and deuterium targets have been unable to pin down the high x behavior of $d(x)/u(x)$. An analysis by Bodek and Yang [15] indicated that the $d(x)/u(x)$ quark ratio approaches 0.2 as $x \rightarrow 1$. However global, QCD analyzes of experimental results, such as the CTEQ fits [16], do not indicate the need for this higher value of $d(x=1)/u(x=1)$.

The measurement of quark densities at high- x_{Bj} is closely related to the question of the leading power corrections known as “higher twist effects”. The n^{th} order higher twist effects are proportional to $1/Q^{2n}$ and reflect the fact that quarks have transverse momentum within the nucleon and that the probe becomes larger as Q^2 decreases, thus increasing the probability of multi-quark participation in an interaction. As was the case with the d/u ratio, different analyzes of higher twist corrections in current data leave some unresolved issues that would benefit from new experimental information. Recent work by Yang and Bodek [17] seems to indicate that what has been measured as “higher-twist” in charged lepton scattering analysis is essentially accounted for by increasing the order (NNLO) of

the perturbative QCD expansion used in the analysis.

The only actual measurements of a higher-twist term in neutrino experiments have been two low-statistics bubble chamber experiments: in Gargamelle [18] with freon and in BEBC [19] with NeH_2 . Both bubble chamber analyzes are complicated by nuclear corrections at high- x . However, both analyzes found a twist-4 contribution that is smaller in magnitude than the charged lepton production analysis and, most significantly, is preferentially negative.

There are several indications that current parameterizations of the pdfs are **not** correct at high x . Drell-Yan pair production off hydrogen and deuterium measured by Fermilab experiment E866 [20] compared to the latest CTEQ global fits, CTEQ6 [21], indicates that the valence distributions are **overestimated** at high- x_{Bj} . This is in direct contrast to a recent NuTeV neutrino results [22] which indicate that the valence distributions are **underestimated** at high x . The NuTeV measurements of $F_2(x)$ deviate in the positive direction from the CCFR values for $F_2(x)$, currently in contemporary global fits such as CTEQ and MRST, as x increases from 0.35, as shown in Figure 6. The NuTeV measurements at $x = 0.65$ are 20% higher than the CCFR values for ν and close to 30% higher for $\bar{\nu}$, although with larger uncertainties. Since both CCFR and NuTeV used the same detector, the difference is not attributable to different nuclear effects. The NuTeV analysis is now in the process of understanding the difference between the NuTeV and CCFR high- x values of $F_2(x)$.

Efforts are underway to understand how the $d(x)/u(x)$ ratio enters into the experimental comparison just discussed. The quark flavor involvement of Drell-Yan scattering, measured in E866, approaches $4u(x) + d(x)$ as $x_{beam} \rightarrow 1.0$. This would tend to indicate that $u(x)$ is overestimated and that $d(x)/u(x)$ is underestimated as $x \rightarrow 1.0$. However, full radiative corrections are only now being applied to the E866 results and the still-unresolved deuterium nuclear corrections have not been applied to either the E866 results or the deuterium data in the global fits. The large sample of high x events in this experiment would certainly help understand these results.

As just mentioned, a major reason that the $d(x)/u(x)$ ratio is not better known is the difficulty of accessing the structure of the neutron, due to the absence of free neutron targets, and the substantial theoretical uncertainties associated with extracting information from neutrons bound in nuclei. To overcome this problem, the BONUS experiment at Jefferson Lab [23] has been approved to measure the inclusive electron scattering cross section on an almost free neutrons using the CEBAF Large Acceptance Spectrometer (CLAS) and a novel recoil detector with low momentum threshold for protons and high rate capability. This detector will allow tagging of slow backward-moving spectator protons with momentum as low as 70 MeV/c in coincidence with the scattered electron in the reaction $D(e, e'p_s)X$. This will ensure that the electron scattering took place on an almost free neutron, with its initial four-momentum inferred from the observed spectator proton spectrum. These measurements will unambiguously provide neutron structure measurements, which will thereby also disclose which of the available models best describe for instance, on-shell

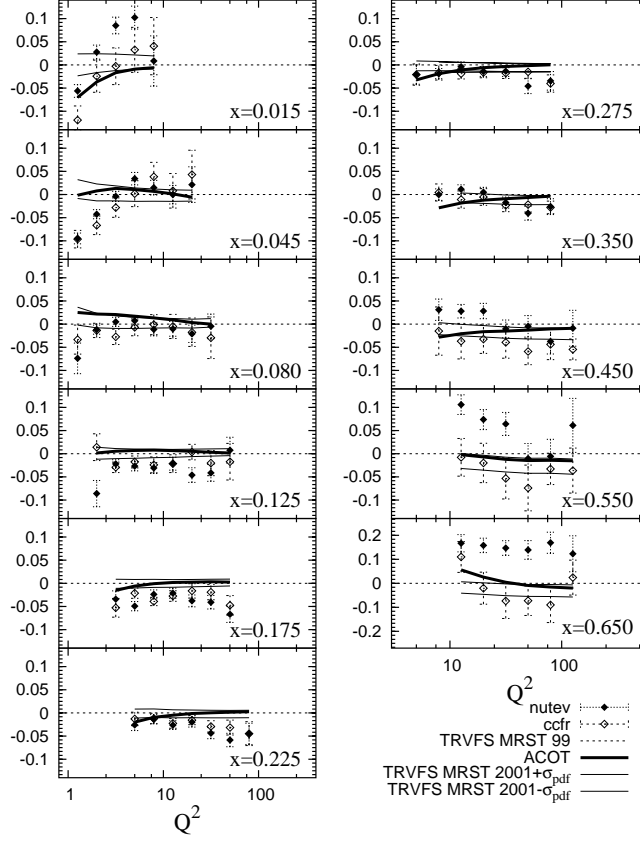


Figure 6: F_2 data compared to fits, from [22]. Shown is $(F_2 - F_2^{model})/F_2^{model}$

extrapolation for neutrons in nuclei. This latter information will be extremely useful to the successful extraction of nucleon structure information from MINER ν A.

We stress here that the BONUS experiment at Jefferson Lab will provide complementary information to the proposed MINER ν A measurements, overlapping in kinematics, and on a complementary time scale. The BONUS and MINER ν A experiments in combination will make a great advance on most of the questions in large x nucleon structure, parton distributions, and medium modifications in the upcoming decade. BONUS will provide vital input regarding the extraction of neutron information from nuclei, while MINER ν A can uniquely provide flavor decomposition information.

The ratio of neutron to proton neutrino structure functions at large x from neutrino scattering will be a particularly interesting MINER ν A measurement. Here, similar valence quark dynamics as in charged lepton scattering are probed, but with different sensitivity to quark flavors. At the hadronic level, quark model studies reveal quite distinct patterns of resonance transitions to the lowest-lying positive and negative parity multiplets of SU(6) [7, 24, 25, 26]. The contributions of the $N \rightarrow N^*$ transition matrix elements to the F_1

and g_1 structure functions of the proton and neutron in the SU(6) quark model may be summed over the $N \rightarrow N^*$ transitions, and yield the expected SU(6) quark-parton model results, providing an explicit confirmation of duality. On the other hand, some modes of spin-flavor symmetry breaking ($\lambda \neq \rho$) yield neutrino structure function ratios which at the parton level are in obvious conflict with those obtained from electroproduction. Neutrino structure function data can therefore provide valuable checks on the appearance of duality and its consistency between electromagnetic and weak probes.

Finally, we also note that MINER ν A will allow for measurements of structure function moments, which have been calculated in lattice QCD. The moments are currently available for $Q^2 = 4 \text{ GeV}^2$, which is within MINER ν A kinematics. Comparisons of the experimental moments with those calculated on the lattice over a range $Q^2 \approx 1\text{--}10 \text{ GeV}^2$ will allow one to determine the size of higher twist corrections and the role played by quark-gluon correlations in the nucleon. For the experimental moments, an appreciable fraction of the strength resides in the nucleon resonance region. Therefore, while a broad range in x is required at fixed Q^2 values to obtain the moments, precise resonance region data are imperative. Since the first moment is an integral over all x , energy resolution uncertainty will play a smaller role in this moment than in the structure function measurements. Lattice calculations of the flavor decomposition of moments of pdfs as well as structure functions at large x and low Q^2 provide a clear role for MINER ν A. For all of these reasons, MINER ν A will provide a vital comparison with results from lattice QCD.

In brief summation, the proposed MINER ν A experiment is uniquely poised to provide a wealth of information crucial to development of understanding beyond a perturbative description of the nucleon. MINER ν A will be the only experiment capable of investigating quark-hadron duality in neutrino scattering. The extraction of parton distribution functions at large x is becoming an increasingly important and controversial topic, in which the vital role of MINER ν A as the only precision neutrino cross section experiment in this regime is unambiguous. MINER ν A can also investigate pdf ratios, structure function moments, large x evolution - all part of a rich physics program at the perturbative to non-perturbative transition region frontier.

References

- [1] W. Melnitchouk, R. Ent, C.E. Keppel, accepted by Physics Reports.
- [2] Sabine Jeschonnek and J.W. Van Orden, Phys. Rev. D **69**, 054006 (2004).
- [3] F. E. Close and Nathan Isgur, Phys. Lett. B **509**, 81-86 (2001).
- [4] R. Ent, C. E. Keppel, I. Niculescu, PRD **62**, 073008 (2000).
- [5] I. Niculescu *et al.*, Phys. Rev. Lett. **85**, 1182-1185 (2000).
- [6] C.E. Carlson and N.C. Mukhopadhyay, Phys. Rev. D **47**, 1737 (1993).

- [7] F.E. Close and F.J. Gilman, Phys. Rev. D **7**, 2258 (1973).
- [8] T. Abdullah and F.E. Close, Phys. Rev. D **5**, 2332 (1972).
- [9] M. Diemoz, F. Ferroni, and E. Longo, Phys. Rev. **130**, 293 (1986).
- [10] R. Belusevic and D. Rein, Phys. Rev. D **38**, 2753 (1988); Phys. Rev. D **46**, 3747 (1992).
- [11] J. Arrington, R. Ent, C.E. Keppel, J. Mammei, and I. Niculescu, nucl-ex/0307012, submitted to Phys. Rev. Lett.
- [12] SPIN0 ref
- [13] G. R. Farrar and D. R. Jackson, Phys. Rev. Lett. **35**, 1416 (1975).
- [14] KUHL ref
- [15] U.K. Yang and A. Bodek, Phys. Rev. Lett. **82**, 2467 (1999).
- [16] Lai:1994bb ref
- [17] A. Bodek and U.K. Yang, Nucl. Phys. B (Proc. Suppl.) 112 70 (2002); **13**, 241 (2000).
- [18] Gargamelletwist ref
- [19] Varvell:1987qu
- [20] J.C. Webb *et al.* [FNAL E866/NuSea Collaboration], hep-ex/0302019.
- [21] See <http://www.phys.psu.edu/~cteq/> for a summary of CTEQ work; H. L. Lai *et al.* [CTEQ Collaboration], Phys. Rev. D **51**, 4763 (1995); H. L. Lai *et al.*, **12**, 375 (2000).
- [22] V. A. Radescu *et al.* [NuTeV Collaboration].
- [23] Jefferson Lab Experiment E03-012, approved.
- [24] F.E. Close and W. Melnitchouk, Phys. Rev. C **68**, 035210 (2003); hep-ph/0302013.
- [25] F.E. Close, F.J. Gilman, and I. Karliner, Phys. Rev. D **6**, 2533 (1972).
- [26] F.E. Close and F.J. Gilman, Phys. Lett. B **38**, 541 (1972).